

# Pairing with Enriched Sound Exposure Restores Auditory Processing Degraded by an Antidepressant

Yuan Cheng,<sup>1,2\*</sup> Ruru Chen,<sup>1,2\*</sup> Bowen Su,<sup>1,2</sup> Guimin Zhang,<sup>1,2</sup> Yutian Sun,<sup>1,2</sup> Pengying An,<sup>1,2</sup> Yue Fang,<sup>1,2</sup> Yifan Zhang,<sup>1,2</sup> Ye Shan,<sup>1</sup>  Étienne de Villers-Sidani,<sup>3</sup> Yunfeng Wang,<sup>4</sup> and Xiaoming Zhou<sup>1,2</sup>

<sup>1</sup>Key Laboratory of Brain Functional Genomics of Ministry of Education, Shanghai Key Laboratory of Brain Functional Genomics, School of Life Sciences, East China Normal University, Shanghai, 200062, China, <sup>2</sup>New York University-East China Normal University Institute of Brain and Cognitive Science, New York University-Shanghai, Shanghai, 200062, China, <sup>3</sup>Department of Neurology and Neurosurgery, Montreal Neurological Institute, McGill University, Montreal, Quebec Canada, and <sup>4</sup>ENT institute and Department of Otorhinolaryngology of Eye & ENT Hospital, NHC Key Laboratory of Hearing Medicine, Fudan University, Shanghai, 200031, China

Antidepressants, while effective in treating depression and anxiety disorders, also induce deficits in sensory (particularly auditory) processing, which in turn may exacerbate psychiatric symptoms. How antidepressants cause auditory signature deficits remains largely unknown. Here, we found that fluoxetine-treated adult female rats were significantly less accurate when performing a tone-frequency discrimination task compared with age-matched control rats. Their cortical neurons also responded less selectively to sound frequencies. The degraded behavioral and cortical processing was accompanied by decreased cortical perineuronal nets, particularly those wrapped around parvalbumin-expressing inhibitory interneurons. Furthermore, fluoxetine induced critical period-like plasticity in their already mature auditory cortices; therefore, a brief rearing of these drug-treated rats under an enriched acoustic environment renormalized auditory processing degraded by fluoxetine. The altered cortical expression of perineuronal nets was also reversed as a result of enriched sound exposure. These findings suggest that the adverse effects of antidepressants on auditory processing, possibly because of a reduction in intracortical inhibition, can be substantially alleviated by simply pairing drug treatment with passive, enriched sound exposure. They have important implications for understanding the neurobiological basis of antidepressant effects on hearing and for designing novel pharmacological treatment strategies for psychiatric disorders.

**Key words:** antidepressant; auditory cortex; cortical plasticity; frequency tuning; inhibition

## Significance Statement

Clinical experience suggests that antidepressants adversely affect sensory (particularly auditory) processing, which can exacerbate patients' psychiatric symptoms. Here, we show that the antidepressant fluoxetine reduces cortical inhibition in adult rats, leading to degraded behavioral and cortical spectral processing of sound. Importantly, fluoxetine induces a critical period-like state of plasticity in the mature cortex; therefore, a brief rearing under an enriched acoustic environment is sufficient to reverse the changes in auditory processing caused by the administration of fluoxetine. These results provide a putative neurobiological basis for the effects of antidepressants on hearing and indicate that antidepressant treatment combined with enriched sensory experiences could optimize clinical outcomes.

Received Oct. 29, 2022; revised Mar. 2, 2023; accepted Mar. 9, 2023.

Author contributions: Y.C., R.C., B.S., G.Z., Y. Sun, P.A., Y.F., Y.Z., and Y. Shan performed research; Y.C., R.C., B.S., G.Z., Y. Sun, P.A., Y.F., Y.Z., Y. Shan, E.d.V.-S., and Y.W. analyzed data; Y.C. and R.C. wrote the first draft of the paper; Y.C., R.C., G.Z., Y. Sun, P.A., Y.F., E.d.V.-S., Y.W., and X.Z. edited the paper; E.d.V.-S., Y.W., and X.Z. wrote the paper; X.Z. designed research.

This work was supported by National Natural Science Foundation of China 32161160325, 321711134, and 82071043; National Science and Technology Innovation 2030 Major Program 2022ZD0204804; Project of Shanghai Science and Technology Commission 21490713200; Program of Introducing Talents of Discipline to Universities B16018; Joint Fund for Medicine and Health 2022JKXYD08001; and New York University-East China Normal University Institute of Brain and Cognitive Science at the New York University-Shanghai matching fund.

\*Y.C. and R.C. contributed equally to this work.

The authors declare no competing financial interests.

Correspondence should be addressed to Xiaoming Zhou at xzmzhou@bio.ecnu.edu.cn.

<https://doi.org/10.1523/JNEUROSCI.2027-22.2023>

Copyright © 2023 the authors

## Introduction

Antidepressants, such as fluoxetine, are widely used to treat depression and anxiety disorders. However, it has been clinically reported that chronic exposure to antidepressants has adverse side effects on sensory (particularly auditory) processing, eliciting hearing disorders, including tinnitus and auditory hallucinations (Oranje et al., 2011; Pattyn et al., 2016; Zhong et al., 2021). These negative effects of antidepressants on hearing are acknowledged factors for psychiatric disorders and are argued to exacerbate psychiatric symptoms (Pattyn et al., 2016; Blazer and Tucci, 2019). While recent studies in rodent models have also demonstrated antidepressant-induced auditory signature deficits

(Simpson et al., 2011; Dringenberg et al., 2014; Ampuero et al., 2019; Pan et al., 2021), their neurologic basis remains largely unknown.

Previous studies on the auditory system have documented an early, several day-long postnatal epoch (i.e., a critical period), during which cortical representation and response selectivity can be remodeled on a large scale merely by passive exposure to sound stimuli (de Villers-Sidani et al., 2007; Insanally et al., 2009; Pysanenko et al., 2018; Nakamura et al., 2020; Svobodová Burianová and Syka, 2020). Beyond this period, cortical modification requires sound input that carries behavioral significance (i.e., behavioral context with attention or reward) (Recanzone et al., 1993; Polley et al., 2006; Zhou and Merzenich, 2009; Zhang et al., 2013; Cheng et al., 2017, 2020). Accordingly, our earlier studies have shown that developmentally degraded cortical processing can be restored in adulthood by auditory training rather than passive sound exposure (Zhou and Merzenich, 2009; Zhu et al., 2016; Liu et al., 2019). While studies have reported that antidepressants reactivate critical period-like plasticity in the adult visual cortex of rodents (Maya Vetencourt et al., 2008; Steinzeig et al., 2019), no similar investigations have been conducted so far on the auditory cortex, which is also a paradigmatic model for plasticity studies of cortical networks. Thus, whether degraded auditory processing can be renormalized through passive sound exposure in the antidepressant-treated mature brain remains to be tested.

Using adult rats as a research model, we first documented the physiological changes in the primary auditory cortex (A1) following chronic fluoxetine treatment and their possible effects on behavioral outcomes. We then investigated whether fluoxetine might induce juvenile-like plasticity in the mature cortex and therefore renormalize drug-altered behavioral and cortical processing, if any, by simply pairing the treatment with enriched sound exposure. Finally, we quantified changes in cortical inhibition accompanying these postexposure effects to elucidate the mechanisms underlying fluoxetine exposure.

## Materials and Methods

All procedures complied with National Institutes of Health standards and were approved by the Institutional Animal Care and Use Committee of East China Normal University. Efforts were made to minimize animal suffering and the number of animals used in the experiments.

**Animal preparation.** Female Sprague Dawley rats, aged 8 weeks, were randomly assigned to either the fluoxetine or water condition. As described previously (Maya Vetencourt et al., 2008), fluoxetine (fluoxetine hydrochloride, Sigma) was dissolved in the drinking water at 200 mg/l and was available *ad libitum*. The control animals received drinking water without fluoxetine. All rats were given free access to food and drinking water under a 12 h light/12 h dark cycle. The researcher remained blind to the group identity of the animals.

**Sound exposure.** Rats in a cage (35 × 22 × 20 cm, length × width × height) were placed in a sound-shielded test chamber for passive sound exposure. The stimuli for tone exposure were pulsed 7 kHz tone pips (50 ms duration with 5 ms ramps) that were delivered at 5 pulses per second (pps) with an intensity of 65 dB sound pressure level (SPL) measured at the center of the cage. There was a 1 s interval of silence between every 5 pulses to minimize adaptation effects. The stimuli for enriched sound exposure were pulse trains with a duration of 1 s that contained 2, 5, 10, or 15 tone pips (50 ms duration with 5 ms ramps). The frequency of each tone pip in the pulse train was set at 1.5, 2.3, 3.5, 5.3, 8.1, 12.3, 19, or 29 kHz. These pulse trains with different frequencies and repetition rates were randomly delivered at 65 dB SPL. Again, there was a 1 s interval of silence between each train presented.

**Open field test.** The apparatus for the open field test was a rectangular box (42 × 42 × 37 cm, length × width × height). During the test, the

rats were placed at the center of the box facing the wall and were left to freely explore over a 10 min period. The total distance traveled was analyzed using a True-Scan System (Coulbourn Instruments). The box was wiped clean with 75% ethanol after each test.

**Elevated zero-maze test.** The elevated zero-maze is an annular platform (5.5 cm width) with an outer diameter of 92 cm divided into two open arms and two opposite closed arms. While the closed arms were enclosed by side walls 20 cm in height, there were no walls for the open arms. The apparatus was elevated 50 cm above the floor. During the test, the rats were placed into one of the open arms facing the closed arm and allowed to freely explore the maze. The behavior of each rat was recorded with a digital camera and analyzed using an ANY-maze system (Stoelting). The maze was wiped clean with 75% ethanol after each test.

**Sound frequency discrimination test.** The behavioral task was conducted in a wire-mesh cage (20 × 20 × 18 cm, length × width × height) enclosed within a sound-attenuating chamber. The acoustic stimuli used were 50 ms tone pips with a 5 ms rise-decay time at 60 dB SPL. The rats were first trained to discriminate a target tone (8 kHz) from a nontarget tone (4 kHz; i.e., one-octave separation from 8 kHz). Only one tone with a specific frequency was presented in each trial. The rats were rewarded for making a go response within a limited time window after the presentation of a target tone. When the animals achieved steady performance scores, sound frequency discrimination was tested on the next day by randomly setting the frequency of the nontarget tone to 7, 6.1, 5.3, 4.6, or 4 kHz (i.e., 0.2, 0.4, 0.6, 0.8, or 1 octave separation from 8 kHz, respectively). The target tone was always 8 kHz during the test.

The behavioral test and data acquisition were controlled by an input and output system consisting of a speaker, photo-beam detector, food dispenser, sound card, and house light (Med Associates). In each trial, a rat's behavioral state could be classified as either a go or a no-go response. The rats were in a go state when the photo-beam of the nose-poke device was interrupted (i.e., a nose-poke response). All other states were considered no-go. For a given trial, the rats could elicit one of five reinforcement states. The first four states were given by the combinations of responses (go or no-go) and stimulus properties (target or nontarget). A go response within 3 s of a target was scored as a hit; a failure to respond within this time window was scored as a miss. A go response within 3 s of a nontarget was scored as a false-positive, and the absence of a response was scored as a withhold. The fifth state, false-alarm, was defined as a go response that occurred  $\geq 3$  s after stimulus presentation. While a hit triggered the delivery of a 45 mg food pellet (BioServe) as a reward, a miss, false-positive, or false-alarm initiated a 9 s time-out during which the lights were turned off and no stimuli were presented. A withhold, however, resulted in neither a reward nor a time-out.

The behavioral discrimination of each rat was quantified as a performance score:  $H - F \times H$  (expressed as a percentage), where  $H$  is the hit rate = the number of hits/the number of target trials and  $F$  is the false-positive rate = the number of false-positives/the number of nontarget trials (Rybalko et al., 2010; Zhu et al., 2014; Tang et al., 2022).

**Auditory brainstem response (ABR) and cortical response recording.** As described in our earlier studies (Cheng et al., 2020, 2022; Tang et al., 2022), the recording was conducted in a shielded, double-walled sound room. The rats were anesthetized with an intraperitoneal injection of sodium pentobarbital (50 mg/kg body weight). A state of areflexia was maintained with supplemental doses of 8 mg/ml dilute pentobarbital injected intraperitoneally during the recording. The animal's body temperature was monitored using a rectal probe and maintained at  $\sim 37^\circ\text{C}$  using a feedback-controlled heating blanket.

For recording the ABR, tone pips (3, 10, 15, or 20 kHz) at different intensities were delivered to the ear through a calibrated earphone with a sound tube positioned inside the external auditory meatus. The ABR was measured by placing three electrodes subdermally at the scalp midline, posterior to the stimulated ear, and on the midline of the back 1–2 cm posterior to the neck of the animal. The ABR threshold was defined as the lowest sound intensity capable of eliciting a response pattern characteristic of that seen at higher intensities.

For cortical recording, the animal was anesthetized and the skull was secured in a head holder, leaving the ears unobstructed. The auditory cortex was surgically exposed and the dura was resected. The cortical

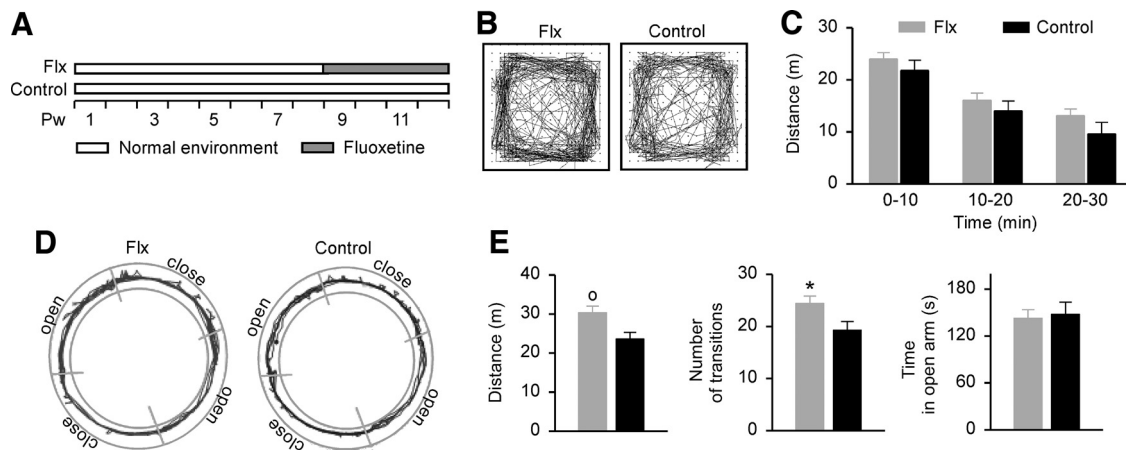


**Figure 1.** Open field and elevated zero-maze tests. **A**, Experimental timelines for the Flx and age-matched control rats. Pw, Postnatal weeks. **B**, Sample movement traces of an Flx rat and a control rat in the open field test. **C**, Comparisons of the average distances traveled during the 10, 20, and 30 min periods between the Flx ( $n = 9$ ) and control ( $n = 9$ ) rats in the open field test. Error bars indicate SEM. **D**, Sample movement traces of an Flx rat and a control rat in the elevated zero-maze test. **E**, Comparisons of the average distance traveled (left), number of transitions between the open and closed arms (middle), and time spent in the open arm (right) between the Flx ( $n = 8$ ) and control ( $n = 9$ ) rats in the elevated zero-maze test.  $^*p < 0.05$ .  $^{\circ}p < 0.01$ .

responses were recorded using parylene-coated tungsten microelectrodes (1–2 M $\Omega$  at 1 kHz; FHC). Acoustic stimuli were delivered to the contralateral ear relative to the recording site through a calibrated earphone with a sound tube positioned inside the external auditory meatus. At each recording site, the microelectrode was lowered orthogonally into the cortex to a depth of  $\sim 450$ – $550$   $\mu\text{m}$  (layers 3/4) (Games and Winer, 1988; Roger and Arnault, 1989) to record the evoked spikes of a neuron or a small cluster of neurons.

The frequency tuning curves were reconstructed by presenting pure tones (25 ms duration) of 50 frequencies (1–30 kHz) at eight sound intensities (0–70 dB SPL in 10 dB increments) in a random, interleaved sequence at a rate of 2 pps. The characteristic frequency (CF) of a cortical site was defined as the frequency at the tip of the V-shaped tuning curve. For flat-peaked tuning curves, the CF was defined as the midpoint of the plateau at the threshold. For tuning curves with multiple peaks, the CF was defined as the frequency at the most sensitive tip (i.e., the tip with the lowest threshold). The response bandwidths that were 20 dB above the threshold of the tuning curves (BW20s) were measured for all recording sites.

As previously described (Rutkowski et al., 2003; Polley et al., 2006, 2007), the A1 was identified based on the unique rostral-to-caudal tonotopy and reliable neuronal responses to tone pips of selective frequencies. To generate A1 maps, Voronoi tessellation (a MATLAB routine; The MathWorks) was performed to create tessellated polygons with electrode penetration sites at their centers. Each polygon was assigned the characteristic (i.e., the CF) of the corresponding penetration site. In this way, every point on the surface of the auditory cortex was linked to the characteristic that was experimentally derived from a sampled cortical site closest to this point.

Software packages SigCal, SigGen, BioSig, and Brainware (Tucker-Davis Technology) were used to calibrate the earphone, generate acoustic stimuli, monitor the response properties online, and store the data for offline analysis, respectively.

**Immunohistochemistry.** As in our earlier studies (Cheng et al., 2020, 2022), the rats that received a lethal dose of pentobarbital (85 mg/kg body weight) were perfused intracardially with saline solution followed by 4% PFA in 0.1 M potassium PBS, pH 7.2. The brains were removed and placed in the same fixative containing 20% sucrose for 12–24 h. The fixed material was sliced in the coronal plane on a freezing microtome (Leica CM3050 S, Leica Microsystems) at a thickness of 40  $\mu\text{m}$ . The free-floating sections were preincubated in a blocking solution to suppress nonspecific binding. The sections were then incubated at 4°C for 12 h with anti-parvalbumin (anti-PV; 1:1000, Sigma) and fluorescein *Wisteria floribunda* lectin (1:400, Vector), and at 37°C for 1 h with the secondary antibody (1:400, Invitrogen). Samples from the different groups of rats were always processed together during the immunostaining procedures

to limit variations related to antibody penetration, incubation time, and the post-sectioning condition of the tissue.

Fluorescence images were acquired using a Leica DM4000 B (Leica Microsystems) epifluorescent microscope equipped with a Leica DFC450 C digital camera (Leica Microsystems). ImageJ (National Institutes of Health) was used for the quantitative analysis of neuron densities in the different cortical layers. To quantify the fluorescence intensity, a horizontal line was drawn in the middle of an identified neuron. ImageJ was then used to analyze the fluorescence intensity along that line to obtain a fluorescence-distance function. The highest intensity on this curve was chosen as the fluorescence intensity of the neuron.

**Experimental design and statistical analysis.** Behavioral, electrophysiological, and immunohistochemical data were recorded as described above and compared between different groups of rats to evaluate the fluoxetine effects on cortical processing. In addition, a basic index of critical period plasticity (i.e., tone-specific enlargement in A1 representation resulting from passive sound exposure) was determined to investigate the plasticity status of A1 following fluoxetine treatment. Finally, fluoxetine treatment was paired with enriched sound exposure to study the reversal effect on drug-degraded cortical processing.

Data are presented as mean  $\pm$  SEM. Statistical analysis was conducted using unpaired Student's *t* test or ANOVA with Student-Newman-Keuls *post hoc* test. In addition, the cumulative distributions of data from different groups were compared with the Kolmogorov–Smirnov test. Differences were considered statistically significant at  $p < 0.05$ .

## Results

The rats were exposed to fluoxetine dissolved in drinking water over a 4 week period beginning at postnatal week 8 (Fig. 1A). These rats were thereafter referred to as the fluoxetine-treated (Flx) rats. In concordance with earlier studies (Thompson et al., 2004; Guirado et al., 2012), chronic fluoxetine treatment produced a moderate decrease in weight gain compared with the age-matched control rats reared under standard housing conditions ( $240.8 \pm 3.3$  g for the Flx rats vs  $251.8 \pm 3.8$  g for the control rats; unpaired *t* test,  $t_{(22)} = 2.18$ ,  $p = 0.04$ ). In addition, the average distances traveled by the Flx rats for locomotor activities during the different test periods were all longer than those traveled by the control rats in the open field test, although the differences did not reach statistical significance (Fig. 1B,C; two-way ANOVA,  $F_{(1,48)} = 3.65$ ,  $p = 0.062$ ). The elevated zero-maze test also revealed that the distance traveled by the Flx rats was longer than that traveled by the control rats (Fig. 1D,E, left; unpaired *t* test,  $t_{(15)} = 2.95$ ,  $p = 0.0099$ ). The number of transitions between

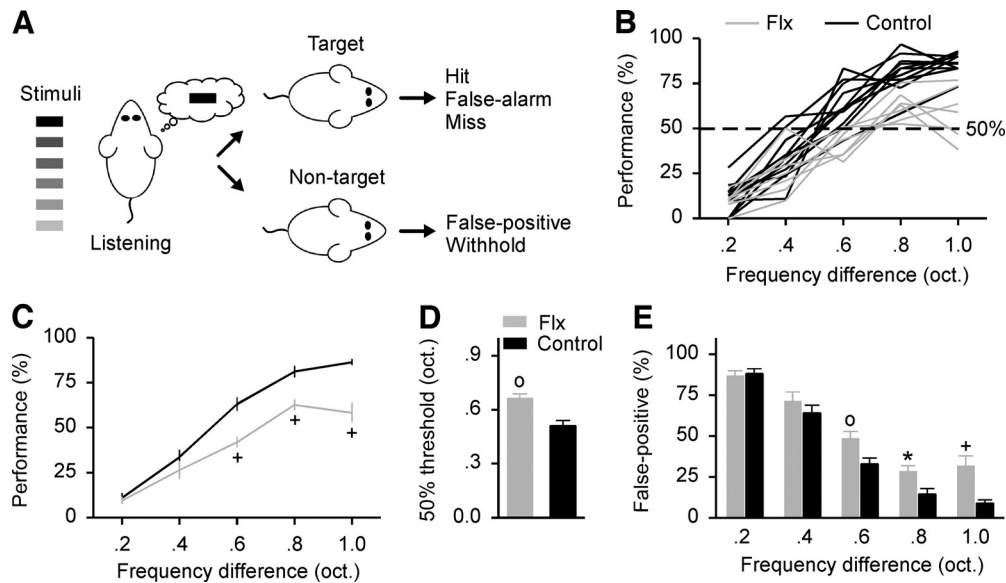


**Figure 2.** Behavioral performance in the sound frequency discrimination task. **A**, Schematic of the sound frequency discrimination task. Only one tone with a specific frequency was presented in each trial during the test. Each animal needed to identify a target tone with a frequency of 8 kHz from a set of distracter tones with frequencies of 0.2, 0.4, 0.6, 0.8, or 1 octave separation from the target tone to obtain a food reward. **B**, Individual psychometric curves obtained from the Flx ( $n = 7$ ) and control ( $n = 11$ ) rats. Dashed line indicates 50% of the maximal score. **C**, Average psychometric curves for both groups of rats. Error bars indicate SEM.  $^+p < 0.001$ . **D**, Comparison of the discrimination thresholds (determined at a 50% performance score on the psychometric curve) for both groups of rats.  $^{\circ}p < 0.01$ . **E**, Average false-positive rates for both groups of rats.  $*p < 0.05$ .

the open and closed arms was also greater for the Flx rats than for the control rats (Fig. 1E, middle; unpaired  $t$  test,  $t_{(15)} = 2.43$ ,  $p = 0.028$ ). However, no significant difference in the time spent in the open arm of the elevated zero-maze was found between the two groups (Fig. 1E, right; unpaired  $t$  test,  $t_{(15)} = 0.26$ ,  $p = 0.8$ ). These data reflect slightly increased locomotor activities but normal anxiety-related behaviors in the Flx rats compared with the controls.

Next, we evaluated the possible consequences of fluoxetine treatment on sound frequency discrimination performance for the Flx rats versus the control rats (Fig. 2A). All the rats were first trained to detect a large-frequency difference (i.e., a one-octave separation) between a target tone and a nontarget tone. After they achieved steady performance scores, the animals underwent a behavioral test in which the frequency difference between the target and the nontarget was varied from 0.2 to 1 octave in each trial by randomly setting the frequency of the nontarget tone. The psychometric curve for each animal was then obtained by plotting the performance score as a function of the frequency difference between the target and the nontarget (Fig. 2B). As shown in Figure 2C, while the performance scores for both groups of rats increased as the frequency difference increased (two-way ANOVA,  $F_{(4,80)} = 118.17$ ,  $p < 0.001$ ), the values were significantly different between the Flx and control rats (two-way ANOVA,  $F_{(1,80)} = 47.28$ ,  $p < 0.001$ ); that is, the performance scores at frequency differences of 0.6, 0.8, and 1 octave were significantly lower for the Flx than the control rats (Student-Newman-Keuls *post hoc* test, all  $p < 0.001$ ). The discrimination threshold, defined as the frequency difference corresponding to 50% of the maximal performance score on the psychometric curve, was significantly higher in the Flx group than in the control group (Fig. 2D; unpaired  $t$  test,  $t_{(16)} = 3.91$ ,  $p = 0.0012$ ). Further analysis revealed that the hit rates during the test were comparable between the two groups of rats ( $90.6 \pm 1.9\%$  for the Flx rats vs  $93.8 \pm 1.5\%$  for the controls; unpaired  $t$  test,  $t_{(16)} = 1.55$ ,  $p = 0.14$ ). However, the fluoxetine treatment had a significant effect on the false-positive rates (Fig. 2E; two-way ANOVA,

$F_{(1,80)} = 22.86$ ,  $p < 0.001$ ) such that the values at frequency differences of 0.6, 0.8, and 1 octave were significantly higher for the Flx than for the control rats (Student-Newman-Keuls *post hoc* test,  $p = 0.005$  at a frequency difference of 0.6 octaves,  $p = 0.012$  at a frequency difference of 0.8 octaves, and  $p < 0.001$  at a frequency difference of 1 octave). These results indicate that fluoxetine treatment degrades the rats' performance in a sound frequency discrimination task.

Earlier studies have shown that peripheral hearing alterations also affect auditory-related behavioral performance (Riley et al., 2021). The ABR is an evoked potential indicator of auditory activity in the auditory nerve and subsequent fiber tracts and nuclei within the auditory brainstem pathways. It provides information about peripheral hearing status and the integrity of brainstem pathways (Zhou et al., 2006; Cheng et al., 2022). To ensure that the degraded performance of the Flx rats in the sound frequency discrimination task could not simply be because of changes in hearing sensitivity after fluoxetine treatment, we recorded the ABRs for both the Flx and control rats (Fig. 3A,B). As shown in Figure 3C, the ABR thresholds recorded from the Flx rats at different frequencies were all comparable to those recorded from the control rats (two-way ANOVA,  $F_{(1,68)} = 0.04$ ,  $p = 0.84$ ). In addition, no significant differences in the ABR latencies of waves I and IV (Fig. 3D; two-way ANOVA,  $F_{(1,68)} = 1.1$ ,  $p = 0.30$  for wave I;  $F_{(1,68)} = 1.94$ ,  $p = 0.17$  for wave IV) or in the wave IV/I amplitude ratios (Fig. 3E; two-way ANOVA,  $F_{(1,68)} = 1.93$ ,  $p = 0.14$ ) were found between the Flx and control rats. Thus, fluoxetine treatment has little impact on peripheral hearing sensitivity.

However, highly significant differences in frequency response selectivity between the Flx and control rats were documented in cortical field A1s. As shown in Figure 4A, B, cortical frequency selectivity was examined by constructing frequency tuning curves for neurons in A1. The CFs and bandwidths 20 dB above the threshold (i.e., BW20s) were then determined. At first glance, cortical field A1s in both the Flx and control rats were relatively tonotopically organized, with the isofrequency bands oriented

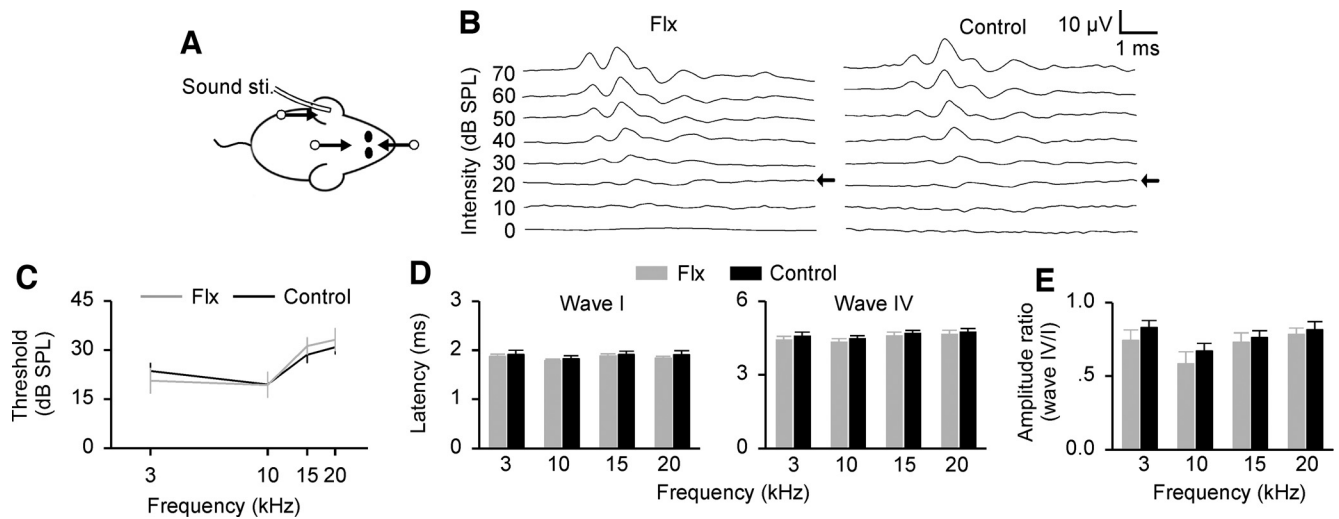


**Figure 3.** Thresholds, wave latencies, and relative wave amplitudes of the ABRs. **A**, Schematic of the experimental setup for ABR recording. The acoustic stimuli were delivered to the ear through a calibrated earphone with a sound tube positioned inside the external auditory meatus. The ABR was recorded by placing three electrodes (indicated by the arrows) subdermally at the scalp midline, posterior to the stimulated ear, and on the midline of the back 1–2 cm posterior to the neck of the animal. **B**, ABR patterns of an Flx rat and a control rat determined with tone pips of 10 kHz. The ABR threshold (arrows) was defined as the lowest sound intensity capable of eliciting a response pattern characteristic of that seen at higher intensities. **C**, ABR thresholds tested at different frequencies for the Flx ( $n = 8$ ) and control ( $n = 11$ ) rats. Error bars indicate SEM. **D**, ABR latencies of waves I (left) and IV (right) for the Flx and control rats. **E**, Relative wave amplitudes (wave IV/I amplitude ratios) for the Flx and control rats.

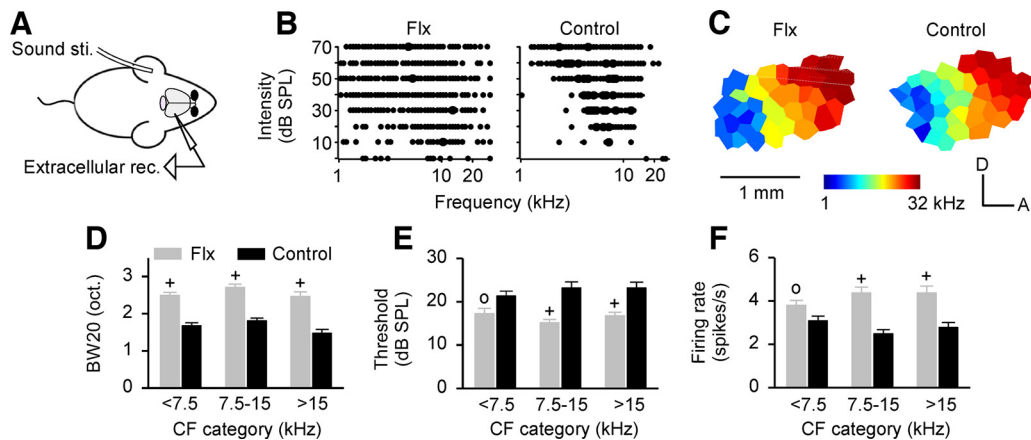


**Figure 4.** Cortical frequency response selectivity. **A**, Schematic of the experimental setup for cortical extracellular recording. **B**, Representative examples of frequency tuning curves of neurons recorded in cortical field A1s of an Flx rat and a control rat. **C**, Representative cortical CF maps of an Flx rat and a control rat. The color of each polygon in these maps represents the CF of the neurons recorded at that site (see the color scales). A, Anterior; D, dorsal. **D**, Average BW20s of cortical neurons recorded in the Flx rats (232 recording sites from 6 animals) and control rats (235 recording sites from 7 animals) for each of the three CF ranges. Error bars indicate SEM.  $^+p < 0.001$ . **E**, Average response thresholds of cortical neurons recorded in the Flx and control rats.  $^{\circ}p < 0.01$ . **F**, Spontaneous firing rates of cortical neurons recorded in the Flx and control rats.

approximately orthogonal to a systematic rostrocaudal frequency representation gradient (Fig. 4C). Further analysis confirmed that the distribution of all CFs recorded from the Flx rats was comparable to that recorded from the control rats (Kolmogorov–Smirnov test,  $p = 0.31$ ). However, neurons all across A1 in the Flx rats responded less selectively (i.e., were less sharply tuned) to sound frequencies than the neurons in the control rats, as evidenced by the systematically and significantly increased bandwidths of the tuning curves (Fig. 4D; two-way ANOVA,  $F_{(1,461)} = 187.95$ ,  $p < 0.001$ ). The Student–Newman–Keuls *post hoc* test showed that  $p < 0.001$  for all CF ranges. Interestingly, the response thresholds of A1 neurons recorded in the Flx rats were lower than those recorded in the controls (Fig. 4E; two-way ANOVA,  $F_{(1,461)} = 45.84$ ,  $p < 0.001$ ). The Student–Newman–Keuls *post hoc* test showed that  $p = 0.002$  in the low CF range but  $p < 0.001$  in both the

middle and high CF ranges. However, the spontaneous firing rates of A1 neurons were higher in the Flx rats than in the controls (Fig. 4F; two-way ANOVA,  $F_{(1,461)} = 55.16$ ,  $p < 0.001$ ). The Student–Newman–Keuls *post hoc* test showed that  $p = 0.007$  in the low CF range but  $p < 0.001$  in both the middle and high CF ranges. All these results were further confirmed by comparing the data using the number of animals as the sample size (BW20:  $2.59 \pm 0.06$  oct. for the Flx rats vs  $1.68 \pm 0.03$  oct. for the control rats, unpaired  $t$  test,  $t_{(11)} = 15.4$ ,  $p < 0.0001$ ; threshold:  $16.7 \pm 0.3$  dB SPL for the Flx rats vs  $22.5 \pm 0.8$  dB SPL for the control rats, unpaired  $t$  test,  $t_{(11)} = 6.3$ ,  $p < 0.0001$ ; spontaneous firing rate:  $4.1 \pm 0.13$  spikes/s for the Flx rats vs  $2.9 \pm 0.14$  spikes/s for the control rats, unpaired  $t$  test,  $t_{(11)} = 6.5$ ,  $p < 0.0001$ ).

Fluoxetine has been shown to induce plasticity in the adult visual cortex, resulting in ocular dominance shifts of neurons after monocular deprivation which is otherwise restricted to the

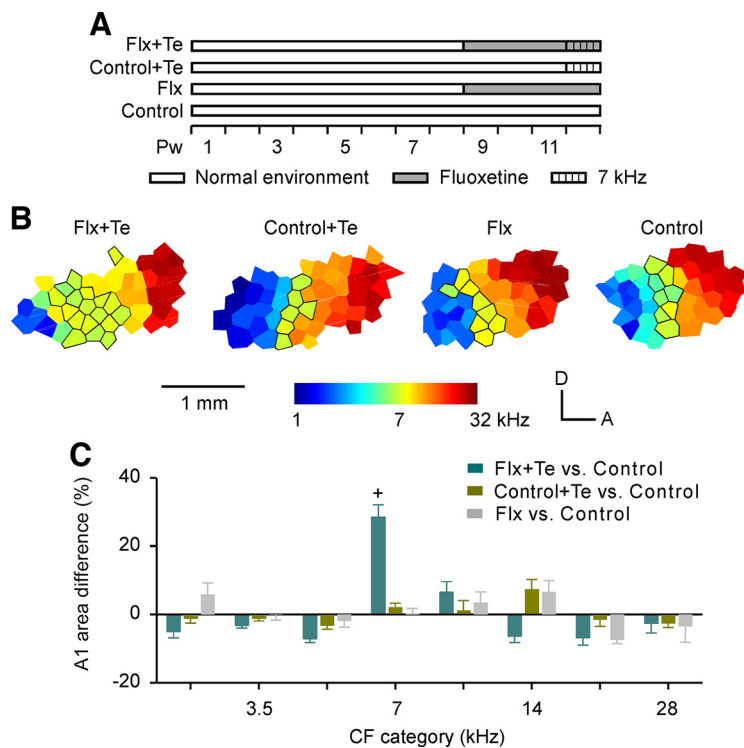


**Figure 5.** Fluoxetine induces critical period-like plasticity in the A1s of adult rats. **A**, Experimental timelines for the Flx+Te, control+Te, Flx, and age-matched control rats. The Flx+Te or control+Te rats, the Flx or control rats were passively exposed to pulsed 7 kHz tones for 1 week. **B**, Representative CF maps obtained from the different groups of rats. Outlined polygons represent recording sites with CFs of  $7 \pm 0.25$  kHz octaves. **C**, Differences in the percentages of A1 areas tuned to the different frequency ranges for the Flx+Te ( $n = 6$ ), control+Te ( $n = 7$ ), and Flx ( $n = 6$ ) rats versus control rats ( $n = 7$ ). Error bars indicate SEM. \* $p < 0.001$  compared with the controls.

critical period (Maya Vetencourt et al., 2008; Steinzeig et al., 2019). We next used a classical model of sound exposure-driven plasticity to determine the plasticity status of A1 in the Flx rats. For this purpose, a subset of the Flx rats was exposed to pulsed 7 kHz tones during the last week of their fluoxetine treatment epoch; these rats were thereafter referred to as the Flx-treated plus tone-exposed rats (Flx+Te rats). In addition, another group of age-matched control rats was exposed to pulsed 7 kHz tones over the same epoch (known thereafter as the control+Te rats). The cortical fields of both groups of rats were then mapped and compared with those of the Flx rats and the controls (Fig. 5A). As shown in Figure 5B, the A1 zone of the control+Te rats that selectively responded to  $7 \pm 0.25$  kHz octaves was comparable to the age-matched controls (control+Te vs control), confirming that their A1s had matured far beyond the normal closure of the critical period window (de Villers-Sidani et al., 2007; Insanally et al., 2009; Zhou et al., 2011). By contrast, in the Flx+Te rats, the A1 zone that selectively responded to  $7 \pm 0.25$  kHz octaves was enlarged by mere sound exposure compared with the control rats (Flx+Te vs control), as seen during the developmental critical period of the rat (de Villers-Sidani et al., 2007; Insanally et al., 2009).

To quantitatively characterize the effects of fluoxetine on A1 frequency representation, the percentages of A1 areas representing each frequency range were averaged within the same experimental group, and the differences between the exposed and control animals were plotted. As shown in Figure 5C, a one-way ANOVA ( $F_{(3,22)} = 48.47$ ,  $p < 0.001$ ) revealed that the average percentage of the A1 area tuned to  $7 \pm 0.25$  kHz octaves in the Flx+Te rats was significantly higher than in the control rats (Student-Newman-Keuls *post hoc* test,  $p < 0.001$ ).

As expected, the average percentages of A1 areas tuned to  $7 \pm 0.25$  kHz octaves in the control+Te and Flx rats were both comparable to those in the control rats (Student-Newman-Keuls *post hoc* test,  $p = 0.70$  for control+Te rats vs control rats and  $p = 0.93$  for Flx rats vs control rats). Since tone-specific enlargement in A1 representation resulting from transient exposure to sound stimuli is a basic index of critical period plasticity, our results indicate that chronic fluoxetine treatment induces critical period-like plasticity in the mature A1s of rats.

Passive sound exposure beyond the critical period does not appear to be sufficient to generate persistent changes in mature A1s (Recanzone et al., 1993; Polley et al., 2006; Zhou and Merzenich, 2009; Zhang et al., 2013; Cheng et al., 2017, 2020). However, inducing critical period-like plasticity in Flx rats makes it possible to remodel their fluoxetine-degraded auditory processing by simply pairing the drug treatment with enriched sound exposure. To test this hypothesis, a group of Flx rats was reared in an enriched acoustic environment during the last week of their fluoxetine treatment epoch (hereafter referred to as the Flx+Eae rats). Their behavioral and cortical processing of sound frequency were then examined and compared with those of age-matched control rats reared under identical conditions over the same epoch (these rats were thereafter referred to as the control+Eae rats), as well as those of the Flx and control rats (Fig. 6A). As shown in Figure 6B, C, a one-way ANOVA ( $F_{(3,28)} = 5.81$ ,  $p = 0.003$ ) revealed that the average discrimination threshold

of the psychometric curves obtained from the Flx+Eae rats significantly decreased compared with the Flx rats (Student-Newman-Keuls *post hoc* test,  $p = 0.003$ ) and was now comparable to that of the control rats (Student-Newman-Keuls *post hoc* test,  $p = 0.27$ ). The average discrimination threshold of the control+Eae rats, however, was substantially similar to that of the controls (Student-Newman-Keuls *post hoc* test,  $p = 0.79$ ). In addition, extracellular recording revealed that the average BW20s of the frequency tuning curves recorded in the Flx+Eae rats were significantly smaller than those in the Flx rats (Fig. 6D,E; two-way ANOVA,  $F_{(3,36)} = 81.09$ ,  $p < 0.001$ ). The Student-Newman-Keuls *post hoc* test showed that  $p < 0.001$  for all CF ranges. These values were again comparable to those recorded in the control rats (Student-Newman-Keuls *post hoc* test,  $p = 0.10$ ,  $p = 0.074$ , and  $p = 0.33$  in the low, middle, and high CF ranges, respectively). As expected, the average BW20s of the control+Eae rats did not differ from those of the control rats (Student-Newman-Keuls *post hoc* test,  $p = 0.052$ ,  $p = 0.46$ , and  $p = 0.20$  in the low, middle, and high CF ranges, respectively). These data show that a week of enriched sound exposure broadly renormalizes the behavioral and cortical processing of sound frequency degraded by fluoxetine treatment.

The status of PV-expressing inhibitory interneurons and the expression of perineuronal nets (PNNs) are both proposed to contribute to neural processing and the regulation of plasticity in cortical networks (Pizzorusso et al., 2002; de Villers-Sidani et al., 2008; Moore and Wehr, 2013; Li et al., 2015; Lensjø et al., 2017; Nguyen et al., 2017; Cheng et al., 2022). To document the cellular and molecular changes at the cortical level that were induced by

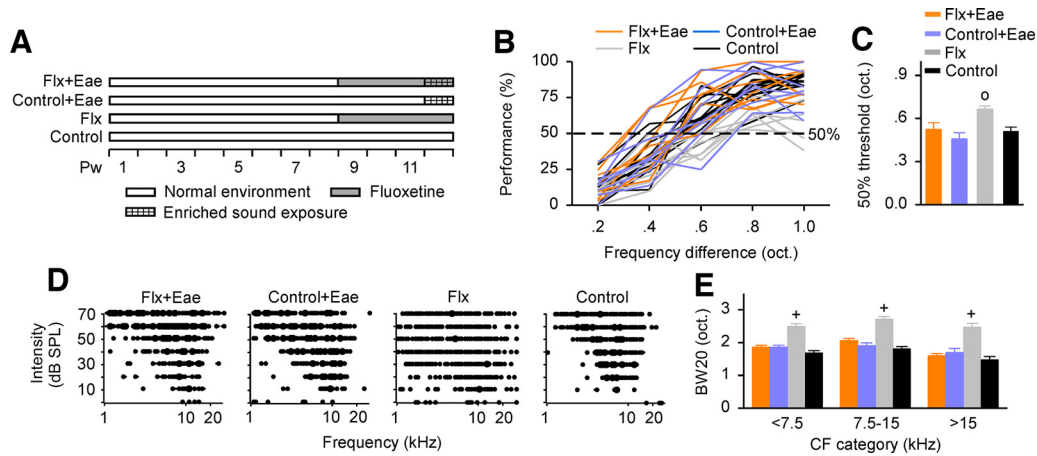


**Figure 6.** Enriched sound exposure renormalizes behavioral and cortical processing degraded by fluoxetine treatment. **A**, Experimental timelines for the Flx+Eae, control+Eae, Flx, and age-matched control rats. The Flx+Eae or control+Eae rats, the Flx or control rats were reared in an enriched acoustic environment for 1 week. **B**, Individual psychometric curves obtained from the Flx+Eae ( $n = 7$ ), control+Eae ( $n = 7$ ), Flx ( $n = 7$ ), and control ( $n = 11$ ) rats. Dashed line indicates 50% of the maximal score. **C**, Comparison of discrimination thresholds (determined at a 50% performance score on the psychometric curve) for the different groups of rats. Error bars indicate SEM.  $^{\circ}p < 0.01$  compared with the controls. **D**, Representative examples of frequency tuning curves of neurons recorded from an Flx+Eae rat, a control+Eae rat, an Flx rat, and a control rat. **E**, Average BW20s of cortical neurons recorded in the Flx+Eae ( $n = 255$  from 7 animals), control+Eae ( $n = 226$  from 6 animals), Flx ( $n = 232$  from 6 animals), and control ( $n = 235$  from 7 animals) rats for each of the three CF ranges.  $^{\circ}p < 0.001$  compared with the controls.

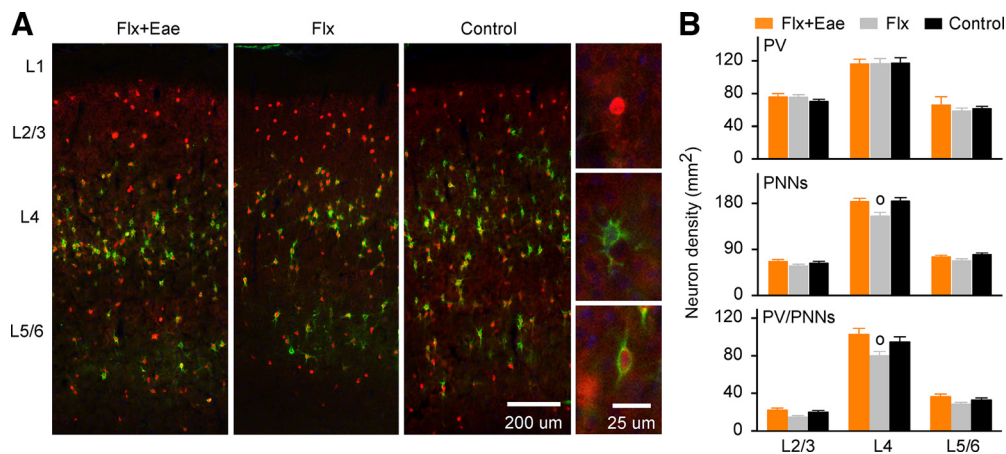


**Figure 7.** Cortical densities of PV-labeled, PNN-labeled, and PV/PNN-colabeled neurons. **A**, Representative photomicrographs of cortical sections for an Flx+Eae rat, an Flx rat, and a control rat. For the experimental timelines of the different groups of rats, see Figure 6A. Left, The cortical layers. Right, Sample PV-labeled (top), PNN-labeled (middle), and PV/PNN-colabeled neurons (bottom). L1, layer 1; L2/3, layers 2/3; L4, layer 4; L5/6, layers 5/6. **B**, Densities of PV-labeled (top), PNN-labeled (middle), and PV/PNN-colabeled neurons (bottom) in different cortical layers of the Flx+Eae rats, Flx rats, and control rats.  $n = 49$  for PV-labeled neurons, 49 for PNN-labeled neurons, and 49 for PV/PNN-colabeled neurons from 5 Flx+Eae rats;  $n = 58$  for PV-labeled neurons, 59 for PNN-labeled neurons, and 58 for PV/PNN-colabeled neurons from 6 Flx rats; and  $n = 59$  for PV-labeled neurons, 60 for PNN-labeled neurons, and 59 for PV/PNN-colabeled neurons from 6 control rats. Error bars indicate SEM.  $^{\circ}p < 0.01$  compared with the controls.

the fluoxetine treatment and their potential reversion to normal by enriched sound exposure, we quantified the expression levels of PV and PNNs in cortical field A1s for the Flx+Eae, Flx, and control rats (Fig. 7A).

Consistent with earlier studies (Nguyen et al., 2017; Fawcett et al., 2019; Reinhard et al., 2019; Cheng et al., 2020, 2022; Aronitz et al., 2021), both PV- and PNN-labeled neurons were distributed more in the middle layer than in the superficial and deep layers of A1. While the fluoxetine treatment had little effect on the densities of PV neurons in the different cortical layers (Fig. 7B, top; two-way ANOVA,  $F_{(2,489)} = 0.40$ ,  $p = 0.67$ ), it did decrease the densities of PNN neurons, particularly in layer 4 (Fig. 7B, middle; two-way ANOVA,  $F_{(2,495)} = 7.81$ ,  $p < 0.001$ ). The Student-Newman-Keuls *post hoc* test showed that  $p = 0.004$  for layer 4, but  $p = 0.33$  for layers 2/3 and  $p = 0.11$  for layers 5/6. Enriched sound exposure significantly increased the density of

PNN neurons in layer 4 of the Flx+Eae rats compared with the Flx rats (Student-Newman-Keuls *post hoc* test,  $p = 0.003$ ); thus, the neuron density in layer 4 for the Flx+Eae rats was substantially similar to that for the control rats (Student-Newman-Keuls *post hoc* test,  $p = 0.92$ ). Since PNNs in the cortex typically form around PV neurons (Favuzzi et al., 2017; Aronitz et al., 2021), we also quantified the densities of PV/PNN-colabeled neurons for the different groups of rats. As shown in Figure 7B (bottom), a two-way ANOVA ( $F_{(2,489)} = 11.08$ ,  $p < 0.001$ ) revealed that the density of PV/PNN neurons for the Flx rats was significantly lower than that for the control rats in cortical layer 4 (Student-Newman-Keuls *post hoc* test,  $p = 0.001$ ). Once again, the density of PV/PNN neurons in the Flx+Eae rats was significantly higher than that in the Flx rats (Student-Newman-Keuls *post hoc* test,  $p < 0.001$ ) and was similar to that in the control rats (Student-Newman-Keuls *post hoc* test,  $p = 0.09$ ). The densities of PV/PNN

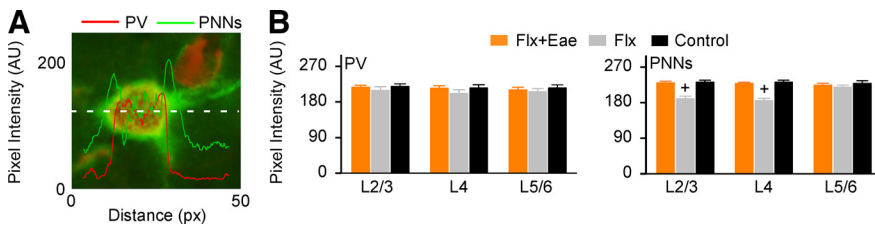


**Figure 8.** Expression intensities of PVs and PNNs for the PV-/PNN-labeled neurons. **A**, Pixel intensities along the horizontal dashed line centered on a PV-/PNN-labeled neuron were measured for PV and PNN expressions. **B**, Expression intensities of PV and PNNs for the Flx+Eae rats, Flx rats, and control rats.  $n = 120$  (40 for each of layers 2/3, 4, and 5/6) from 5 Flx+Eae rats;  $n = 130$  (40 for both layers 2/3 and 4, and 50 for layers 5/6) from 6 Flx rats; and  $n = 137$  (46 for layers 2/3, 47 for layer 4, and 44 for layers 5/6) from 6 control rats.  $^+p < 0.001$  compared with the controls.

neurons in both the superficial and deep cortical layers, however, did not differ among the various groups of rats (Student-Newman-Keuls *post hoc* test, all  $p > 0.22$ ).

For the PV-/PNN-labeled neurons, we further quantified the intensities of expression for both the PV and PNNs (Fig. 8A). As shown in Figure 8B, the intensities of PV expression for the PV/PNN neurons located in the different cortical layers were all comparable among the different groups of rats (two-way ANOVA,  $F_{(2,378)} = 2.12$ ,  $p = 0.12$ ). However, the intensities of PNN expression for the Flx rats were significantly lower than those for the controls, except for neurons in the deep cortical layer (two-way ANOVA,  $F_{(2,378)} = 44.20$ ,  $p < 0.001$ ). The Student-Newman-Keuls *post hoc* test showed that  $p < 0.001$  for both layers 2/3 and layer 4, but  $p = 0.30$  for layers 5/6. The intensities of PNN expression for both layers 2/3, and 4 of the Flx+Eae rats were again significantly higher than those of the Flx rats (Student-Newman-Keuls *post hoc* test, both  $p < 0.001$ ) and were comparable to those of the control rats (Student-Newman-Keuls *post hoc* test,  $p = 0.73$  for layers 2/3 and  $p = 0.67$  for layer 4).

## Discussion

In this study, 2-month-old rats were chronically treated with antidepressant fluoxetine for 4 weeks. At this age, a rat is approaching sexual maturity, and its A1 has matured far beyond the normal closure of the critical period for passive sound exposure-driven plasticity (de Villers-Sidani et al., 2007; Insanally et al., 2009; Zhou et al., 2011). We found that the Flx rats were significantly less accurate when performing a tone-frequency discrimination task compared with the control rats. Their cortical neurons also responded less selectively to sound frequencies, as shown by the larger bandwidths of the frequency tuning curves. The degraded behavioral and cortical spectral processing was accompanied by decreased cortical PNNs, particularly those wrapped around PV-expressing interneurons, indicating a reduction in intracortical inhibition. More importantly, fluoxetine induced a period of sound exposure-driven plasticity in their auditory cortices. Thus, a week of rearing the Flx rats under an enriched acoustic environment substantially renormalized tone-frequency discrimination and cortical spectral selectivity, which had been degraded by the fluoxetine treatment. The cortical expression of the PNNs was also reversed as a result of this passive, enriched sound exposure. Our study thus documents a strong capacity for driving “negative” cortical changes (i.e., decreased frequency tuning and reduced intracortical inhibition) which normally characterize a more immature cortex by chronically exposing adult rats to fluoxetine. The findings that cortical processing moved in the direction of a “more immature” status indicate that fluoxetine promotes cortical plasticity by inducing a critical period-like epoch in the A1s of adult rats.

Cortical inhibition plays an important role in shaping the response properties of neurons in A1, which determine behavioral and perceptual discrimination (J. Wang et al., 2000; Wehr and Zador, 2003; Wu et al., 2008; Li et al., 2014; Seybold et al., 2015; Natan et al., 2017; Liu and Kanold, 2021; Cheng et al., 2022). A mature, functionally differentiated cortex, with its strong and powerful selective inhibitory processes in place, responds with greater selectivity to the stimuli. Conversely, reduced intracortical inhibition, while promoting cortical plasticity (see below), might decrease the frequency selectivity of neurons and

thus degrade the tone-frequency discrimination performance, as observed in the Flx rats. This hypothesis is further strengthened by a positive change in cortical inhibition after enriched sound exposure, which parallels the recovery of cortical and behavioral spectral processing in the Flx+Eae rats. Of note, recent studies have also shown that fluoxetine decreases the complexity of the dendritic arbors and inhibits the LTP induced by theta-burst stimulation of the medial geniculate nucleus in the auditory cortices of adult rats (Dringenberg et al., 2014; Ampuero et al., 2019). These fluoxetine effects recorded in the auditory cortex plausibly also contribute to the altered behavioral performance in the Flx rats. At the same time, most current studies on fluoxetine action have focused on forebrain structures (Maya Vetencourt et al., 2008; Karpova et al., 2011; Ohira et al., 2013; Mikics et al., 2018; Steinzeig et al., 2019). Therefore, whether and how fluoxetine might alter neural processing in the subcortical areas of the adult brain remain to be studied. Our ongoing studies conducted on the auditory midbrain (i.e., the inferior colliculus) are expected to shed light on this question in the near future.

Earlier studies on the auditory system have shown that cortical representation and response selectivity can be substantially remodeled by passive exposure to sound stimuli during the critical period of postnatal development (de Villers-Sidani et al., 2007; Insanally et al., 2009; Pysanenko et al., 2018; Nakamura et al., 2020; Svobodová Burianová and Syka, 2020). Beyond this period, cortical modification requires sound input that carries behavioral significance (Recanzone et al., 1993; Polley et al., 2006; Zhou and Merzenich, 2009; Zhang et al., 2013; Cheng et al., 2017, 2020). In this study, a subset group of Flx rats was passively exposed to enriched sound to further identify the effects of fluoxetine on cortical plasticity. While transient sound exposure had little effect on the behavioral or cortical processing of sound frequency in the control rats, it did evoke significant changes in the fluoxetine-treated adult rats; juvenile-like immature characteristics (i.e., degraded frequency discrimination, reduced cortical frequency selectivity, and decreased cortical PNN expression) were all reversed after sound exposure. Our results therefore again support the conclusion that chronic fluoxetine treatment induces a critical period-like epoch in the auditory cortices of adult rats.

It has been proposed that maturation of inhibition in cortical networks serves as a “brake” for developmental plasticity (Hensch, 2005). Thus, manipulations that reduce intracortical inhibition can promote cortical plasticity in mature brains. For example, a reduction in cortical GABAergic inhibition, either by pharmacological treatment or dark rearing in adult animals, has been shown to reopen a period of stimulus exposure-based plasticity in the visual cortex (Maya Vetencourt et al., 2008; Harauzov et al., 2010).

Similarly, exposing adult rats to continuous white noise restores critical period-like plasticity in the auditory cortex; and again, changes in the GABAergic inhibitory processes have been recorded in parallel with enhanced cortical plasticity (Zhou et al., 2011). More recently, it has been reported that reducing cortical inhibition by the chemogenetic inactivation of PV neurons also reinstates plasticity in the adult mouse auditory cortex (Cisneros-Franco and de Villers-Sidani, 2019). In this study, we found that chronic treatment with fluoxetine decreased the expression of cortical PNNs, resulting in a reduced density of PV-/PNN-colabeled neurons, particularly in the middle layers of the auditory cortex. Similar results have previously been reported in the medial frontal cortex and the BLA of adult animals after fluoxetine treatment (Karpova et al., 2011; Ohira et al., 2013). PNNs are reticular structures composed of extracellular matrix molecules (D. Wang and Fawcett, 2012). In the cortex, PNNs typically accumulate around the soma and proximal dendrites of PV neurons and have been shown to mediate trophic support to these neurons and maintain mature excitatory synaptic contacts onto them (Favuzzi et al., 2017; Fawcett et al., 2019; Aronitz et al., 2021). Thus, fluoxetine-reduced expression of PNNs, particularly those that encapsulate PV neurons, indicates a disruption of the intrinsic properties of these PV neurons and, hence, the reduction of cortical inhibitory networks (as evidenced by reduced spectral tuning and decreased response thresholds of neurons recorded in the fluoxetine-treated A1). We propose that reduced intracortical inhibition resulting from the decline in PNN expression following fluoxetine treatment at least partly contributes to enhanced A1 plasticity in adult rats.

Except for GABAergic inhibition, both glutamatergic excitation and BDNF signaling are also argued to play important roles in regulating or enabling changes in plasticity that express the transition of the brain from its infantile to adult stage (Bracken and Turrigiano, 2009; Zhou et al., 2011). Earlier studies have shown that antidepressant administration regulates glutamatergic transmission and BDNF signaling in the adult brain (Maya Vetencourt et al., 2008; Mikics et al., 2018; Ampuero et al., 2019; Van Dyke et al., 2019). Thus, we cannot rule out the possibility that altered glutamatergic excitation and/or BDNF signaling as a result of fluoxetine treatment also contribute to enhanced plasticity in the mature auditory cortex. Further studies are needed to answer questions as to whether and how these different mechanistic pathways are related to each other while inducing critical period-like plasticity in the adult auditory cortex.

Typical perceptual deficits often manifest as a lateral shift of the psychometric curve. In this study, the Flx rats showed significant behavioral deficits even at the largest frequency difference between the target and nontarget we tested (i.e., at a difference of 1 octave). This result indicates that more large-frequency differences that are perceptually unchallenging for the Flx rats to discriminate may need to be tested in future studies. Furthermore, the discrimination task applied in this study also requires top-down motivation and learning and memory processes to achieve target recognition. While the hit rates of the Flx rats in the behavioral test were comparable to those of the control rats, the false-positive rates were significantly higher at large-frequency differences. In addition to degraded auditory processing, these higher false-positive rates may reflect an over-motivated state for food rewards, impulsivity, or decreased attention. Further studies therefore are needed to distinguish the effects of fluoxetine exposure on auditory discrimination sensitivity versus other nonsensory

factors. Finally, how long the postexposure effects of fluoxetine on behavior and cortical processing last and whether the reversal effects of fluoxetine pairing with enriched sound exposure on auditory processing persist also require further study.

## References

- Ampuero E, Cerda M, Härtel S, Rubio FJ, Massa S, Cubillos P, Abarzúa-Catalán L, Sandoval R, Galaburda AM, Wynken U (2019) Chronic fluoxetine treatment induces maturation-compatible changes in the dendritic arbor and in synaptic responses in the auditory cortex. *Front Pharmacol* 10:804.
- Aronitz EM, Kamermans BA, Duffy KR (2021) Development of parvalbumin neurons and perineuronal nets in the visual cortex of normal and dark-exposed cats. *J Comp Neurol* 529:2827–2841.
- Blazer DG, Tucci DL (2019) Hearing loss and psychiatric disorders: a review. *Psychol Med* 49:891–897.
- Bracken BK, Turrigiano GG (2009) Experience-dependent regulation of TrkB isoforms in rodent visual cortex. *Dev Neurobiol* 69:267–278.
- Cheng Y, Jia G, Zhang Y, Hao H, Shan Y, Yu L, Sun X, Zheng Q, Kraus N, Merzenich MM, Zhou X (2017) Positive impacts of early auditory training on cortical processing at an older age. *Proc Natl Acad Sci USA* 114:6364–6369.
- Cheng Y, Zhang Y, Wang F, Jia G, Zhou J, Shan Y, Sun X, Yu L, Merzenich MM, Recanzone GH, Yang L, Zhou X (2020) Reversal of age-related changes in cortical sound-azimuth selectivity with training. *Cereb Cortex* 30:1768–1778.
- Cheng Y, Tang B, Zhang G, An P, Sun Y, Gao M, Zhang Y, Shan Y, Zhang J, Liu Q, Lai CS, de Villers-Sidani É, Wang Y, Zhou X (2022) Degraded cortical temporal processing in the valproic acid-induced rat model of autism. *Neuropharmacology* 209:109000.
- Cisneros-Franco JM, de Villers-Sidani É (2019) Reactivation of critical period plasticity in adult auditory cortex through chemogenetic silencing of parvalbumin-positive interneurons. *Proc Natl Acad Sci USA* 116:26329–26331.
- de Villers-Sidani E, Chang EF, Bao S, Merzenich MM (2007) Critical period window for spectral tuning defined in the primary auditory cortex (A1) in the rat. *J Neurosci* 27:180–189.
- de Villers-Sidani E, Simpson KL, Lu YF, Lin RC, Merzenich MM (2008) Manipulating critical period closure across different sectors of the primary auditory cortex. *Nat Neurosci* 11:957–965.
- Dringenberg HC, Branfield Day LR, Choi DH (2014) Chronic fluoxetine treatment suppresses plasticity (long-term potentiation) in the mature rodent primary auditory cortex in vivo. *Neural Plast* 2014:571285.
- Favuzzi E, Marques-Smith A, Deogracias R, Winterflood CM, Sánchez-Aguilera A, Mantoan L, Maeso P, Fernandes C, Ewers H, Rico B (2017) Activity-dependent gating of parvalbumin interneuron function by the perineuronal net protein brevican. *Neuron* 95:639–655.e5.
- Fawcett JW, Oohashi T, Pizzorusso T (2019) The roles of perineuronal nets and the perinodal extracellular matrix in neuronal function. *Nat Rev Neurosci* 20:451–465.
- Games KD, Winer JA (1988) Layer V in rat auditory cortex: projections to the inferior colliculus and contralateral cortex. *Hear Res* 34:1–25.
- Guirado R, Sanchez-Matarredona D, Varea E, Crespo C, Blasco-Ibáñez JM, Nacher J (2012) Chronic fluoxetine treatment in middle-aged rats induces changes in the expression of plasticity-related molecules and in neurogenesis. *BMC Neurosci* 13:5.
- Harauzov A, Spolidoro M, DiCristo G, De Pasquale R, Cancedda L, Pizzorusso T, Viegi A, Berardi N, Maffei L (2010) Reducing intracortical inhibition in the adult visual cortex promotes ocular dominance plasticity. *J Neurosci* 30:361–371.
- Hensch TK (2005) Critical period plasticity in local cortical circuits. *Nat Rev Neurosci* 6:877–888.
- Insanally MN, Köver H, Kim H, Bao S (2009) Feature-dependent sensitive periods in the development of complex sound representation. *J Neurosci* 29:5456–5462.
- Karpova NN, Pickenhagen A, Lindholm J, Tiraboschi E, Kulesskaya N, Agústsdtóttir A, Antila H, Popova D, Akamine Y, Bahi A, Sullivan R, Hen R, Drew LJ, Castrén E (2011) Fear erasure in mice requires synergy between antidepressant drugs and extinction training. *Science* 334:1731–1734.

- Lensjø KK, Lepperød ME, Dick G, Hafting T, Fyhn M (2017) Removal of perineuronal nets unlocks juvenile plasticity through network mechanisms of decreased inhibition and increased gamma activity. *J Neurosci* 37:1269–1283.
- Li LY, Ji XY, Liang F, Li YT, Xiao Z, Tao HW, Zhang LI (2014) A feedforward inhibitory circuit mediates lateral refinement of sensory representation in upper layer 2/3 of mouse primary auditory cortex. *J Neurosci* 34:13670–13683.
- Li LY, Xiong XR, Ibrahim LA, Yuan W, Tao HW, Zhang LI (2015) Differential receptive field properties of parvalbumin and somatostatin inhibitory neurons in mouse auditory cortex. *Cereb Cortex* 25:1782–1791.
- Liu J, Kanold PO (2021) Diversity of receptive fields and sideband inhibition with complex thalamocortical and intracortical origin in L2/3 of mouse primary auditory cortex. *J Neurosci* 41:3142–3162.
- Liu X, Wei F, Cheng Y, Zhang Y, Jia G, Zhou J, Zhu M, Shan Y, Sun X, Yu L, Merzenich MM, Lurie DI, Zheng Q, Zhou X (2019) Auditory training reverses lead (Pb)-toxicity-induced changes in sound-azimuth selectivity of cortical neurons. *Cereb Cortex* 29:3294–3304.
- Maya Vetencourt JF, Sale A, Viegi A, Baroncelli L, De Pasquale R, O'Leary OG, Castrén E, Maffei L (2008) The antidepressant fluoxetine restores plasticity in the adult visual cortex. *Science* 320:385–388.
- Mikics É, Guirado R, Umemori J, Tóth M, Biró L, Miskolczi C, Balázsfi D, Zelena D, Castrén E, Haller J, Karpova NN (2018) Social learning requires plasticity enhanced by fluoxetine through prefrontal Bdnf-TrkB signaling to limit aggression induced by post-weaning social isolation. *Neuropsychopharmacology* 43:235–245.
- Moore AK, Wehr M (2013) Parvalbumin-expressing inhibitory interneurons in auditory cortex are well-tuned for frequency. *J Neurosci* 33:13713–13723.
- Nakamura M, Valerio P, Bhumika S, Barkat TR (2020) Sequential organization of critical periods in the mouse auditory system. *Cell Rep* 32:108070.
- Natan RG, Rao W, Geffen MN (2017) Cortical interneurons differentially shape frequency tuning following adaptation. *Cell Rep* 21:878–890.
- Nguyen A, Khaleel HM, Razak KA (2017) Effects of noise-induced hearing loss on parvalbumin and perineuronal net expression in the mouse primary auditory cortex. *Hear Res* 350:82–90.
- Ohira K, Takeuchi R, Iwanaga T, Miyakawa T (2013) Chronic fluoxetine treatment reduces parvalbumin expression and perineuronal nets in gamma-aminobutyric acidergic interneurons of the frontal cortex in adult mice. *Mol Brain* 6:43.
- Oranje B, Wienberg M, Glenthøj BY (2011) A single high dose of escitalopram disrupts sensory gating and habituation, but not sensorimotor gating in healthy volunteers. *Psychiatry Res* 186:431–436.
- Pan W, Pan J, Zhao Y, Zhang H, Tang J (2021) Serotonin transporter defect disturbs structure and function of the auditory cortex in mice. *Front Neurosci* 15:749923.
- Pattyn T, Van Den Eede F, Vanneste S, Cassiers L, Veltman DJ, Van De Heyning P, Sabbe BC (2016) Tinnitus and anxiety disorders: a review. *Hear Res* 333:255–265.
- Pizzorusso T, Medini P, Berardi N, Chierzi S, Fawcett JW, Maffei L (2002) Reactivation of ocular dominance plasticity in the adult visual cortex. *Science* 298:1248–1251.
- Polley DB, Steinberg EE, Merzenich MM (2006) Perceptual learning directs auditory cortical map reorganization through top-down influences. *J Neurosci* 26:4970–4982.
- Polley DB, Read HL, Storaice DA, Merzenich MM (2007) Multiparametric auditory receptive field organization across five cortical fields in the albino rat. *J Neurophysiol* 97:3621–3638.
- Pysanen K, Bureš Z, Lindovský J, Syka J (2018) The effect of complex acoustic environment during early development on the responses of auditory cortex neurons in rats. *Neuroscience* 371:221–228.
- Recanzone GH, Schreiner CE, Merzenich MM (1993) Plasticity in the frequency representation of primary auditory cortex following discrimination training in adult owl monkeys. *J Neurosci* 13:87–103.
- Reinhard SM, Abundez-Toledo M, Espinoza K, Razak KA (2019) Effects of developmental noise exposure on inhibitory cell densities and perineuronal nets in A1 and AAF of mice. *Hear Res* 381:107781.
- Riley JR, Borland MS, Tamaoki Y, Skipton SK, Engineer CT (2021) Auditory brainstem responses predict behavioral deficits in rats with varying levels of noise-induced hearing loss. *Neuroscience* 477:63–75.
- Roger M, Arnault P (1989) Anatomical study of the connections of the primary auditory area in the rat. *J Comp Neurol* 287:339–356.
- Rutkowski RG, Miasnikov AA, Weinberger NM (2003) Characterisation of multiple physiological fields within the anatomical core of rat auditory cortex. *Hear Res* 181:116–130.
- Rybalko N, Suta D, Popelár J, Syka J (2010) Inactivation of the left auditory cortex impairs temporal discrimination in the rat. *Behav Brain Res* 209:123–130.
- Seybold BA, Phillips EA, Schreiner CE, Hasenstaub AR (2015) Inhibitory actions unified by network integration. *Neuron* 87:1181–1192.
- Simpson KL, Weaver KJ, de Villers-Sidani E, Lu JY, Cai Z, Pang Y, Rodriguez-Porcel F, Paul IA, Merzenich M, Lin RC (2011) Perinatal antidepressant exposure alters cortical network function in rodents. *Proc Natl Acad Sci USA* 108:18465–18470.
- Steinzeig A, Cannarozzo C, Castrén E (2019) Fluoxetine-induced plasticity in the visual cortex outlasts the duration of the naturally occurring critical period. *Eur J Neurosci* 50:3663–3673.
- Svobodová Burianová J, Syka J (2020) Postnatal exposure to an acoustically enriched environment alters the morphology of neurons in the adult rat auditory system. *Brain Struct Funct* 225:1979–1995.
- Tang B, Li K, Cheng Y, Zhang G, An P, Sun Y, Fang Y, Liu H, Shen Y, Zhang Y, Shan Y, de Villers-Sidani E, Zhou X (2022) Developmental exposure to bisphenol A degrades auditory cortical processing in rats. *Neurosci Bull* 38:1292–1302.
- Thompson MR, Li KM, Clemens KJ, Gurtman CG, Hunt GE, Cornish JL, McGregor IS (2004) Chronic fluoxetine treatment partly attenuates the long-term anxiety and depressive symptoms induced by MDMA ('Ecstasy') in rats. *Neuropsychopharmacology* 29:694–704.
- Van Dyke AM, Francis TC, Chen H, Bailey AM, Thompson SM (2019) Chronic fluoxetine treatment in vivo enhances excitatory synaptic transmission in the hippocampus. *Neuropharmacology* 150:38–45.
- Wang D, Fawcett J (2012) The perineuronal net and the control of CNS plasticity. *Cell Tissue Res* 349:147–160.
- Wang J, Caspary D, Salvi RJ (2000) GABA-A antagonist causes dramatic expansion of tuning in primary auditory cortex. *Neuroreport* 11:1137–1140.
- Wehr M, Zador AM (2003) Balanced inhibition underlies tuning and sharpens spike timing in auditory cortex. *Nature* 426:442–446.
- Wu GK, Arbuckle R, Liu BH, Tao HW, Zhang LI (2008) Lateral sharpening of cortical frequency tuning by approximately balanced inhibition. *Neuron* 58:132–143.
- Zhang Y, Zhao Y, Zhu X, Sun X, Zhou X (2013) Refining cortical representation of sound azimuths by auditory discrimination training. *J Neurosci* 33:9693–9698.
- Zhong PX, Li IH, Shih JH, Yeh CB, Chiang KW, Kao LT (2021) Antidepressants and risk of sudden sensorineural hearing loss: a population-based cohort study. *Int J Epidemiol* 50:1686–1697.
- Zhou X, Merzenich MM (2009) Developmentally degraded cortical temporal processing restored by training. *Nat Neurosci* 12:26–28.
- Zhou X, Jen PH, Seburn KL, Frankel WN, Zheng QY (2006) Auditory brainstem responses in 10 inbred strains of mice. *Brain Res* 1091:16–26.
- Zhou X, Panizzutti R, de Villers-Sidani E, Madeira C, Merzenich MM (2011) Natural restoration of critical period plasticity in the juvenile and adult primary auditory cortex. *J Neurosci* 31:5625–5634.
- Zhu X, Wang F, Hu H, Sun X, Kilgard MP, Merzenich MM, Zhou X (2014) Environmental acoustic enrichment promotes recovery from developmentally degraded auditory cortical processing. *J Neurosci* 34:5406–5415.
- Zhu X, Liu X, Wei F, Wang F, Merzenich MM, Schreiner CE, Sun X, Zhou X (2016) Perceptual training restores impaired cortical temporal processing due to lead exposure. *Cereb Cortex* 26:334–345.